doi: 10.1175/1520-0426(2000)017<0679:EOTFTP>2.0.CO;2
Journal of Atmospheric and Oceanic Technology: **Vol. 17, No. 5, pp. 679–687.**

Evaluation of Tides from TOPEX/Poseidon in the Bohai and Yellow Seas*

W. J. Teague, P. Pistek, G. A. Jacobs, and H. T. Perkins

Naval Research Laboratory, Stennis Space Center, Mississippi

(Manuscript received 22 January 1999, 12 August 1999)

ABSTRACT

TOPEX/Poseidon (T/P) can provide accurate tide data in the Yellow and Bohai Seas. The accuracy of T/P as a measurement tool for tides in the coastal seas can be evaluated through comparison to data from in situ pressure gauges and coastal tide stations. The effort here is concentrated on the broad continental shelf region of the Yellow and Bohai Seas. Tide coefficients are derived from five years of T/P data for M2, S2, K1, and O1 constituents. These constituents are responsible for about 80% of the tidal variability in the Yellow Sea. The T/P data are compared with two moored pressure gauges deployed along ground tracks and eight coastal tide gauges near the ground tracks. In addition, for internal consistency, the T/P data are compared at seven crossover points. Comparisons with tidal stations are quite good in the Yellow Sea, but not as good in the Bohai Sea. Comparisons of moored pressure gauges with T/P are better than coastal tide station comparisons in terms of tidal amplitude and phase. Crossover point comparisons are best in the Yellow Sea. The T/P data dropouts degrade the coefficient determination within 20 to 35 km of the coast.

1. Introduction Return to TOC

Tides in the Yellow and Bohai Seas are predominately semidiurnal and exhibit considerable spatial variability in both amplitude and phase. There have been numerous tidal charts produced for this region (Ogura 1933 ; Nishida 1980) based on coastal and island measurements. Extensive tide modeling studies (Choi 1988 ; Kantha et al. 1995 ; Blain 1996) have also generated charts of the cotidal and corange lines for the principal semidiurnal (M2 and S2) and diurnal (K1) tides. The M2 semidiurnal tide is dominant (Blain 1997 ; Kantha et al. 1995). Due to the shallow depth of the Yellow Sea and the large amplitudes of the primary tides, compound shallow water or nonlinear tides may have a significant role in the complete tidal picture but have not as yet been quantified. In general, tides off the coast in marginal seas are still not known with confidence.

Satellite altimetry can provide almost global observations of tides (Cartwright and Ray 1990 ; Cartwright and Ray 1994 ; Desai and Wahr 1995). There are now six years of TOPEX/Poseidon (T/P) data available for tide analyses. Numerous methodologies are used in a large number of tide models derived from T/P altimetry (Desai and Wahr 1995

). These tide solutions are more accurate than those produced using Geosat altimeter data due to the different aliasing characteristics and orbit errors (Schlax and Chelton 1994). Here tidal coefficients are derived from T/P data for the four main constituents (M2, S2, K1, and O1) in the Yellow and Bohai Seas. The technique used is based on a least squares fitting technique. The hourly time series of T/P-derived tidal heights are evaluated for selected points along the ground tracks. The T/P tidal heights are then compared with moored pressure gauges in the Yellow Sea interior and coastal tide stations. In addition, T/P data are evaluated at crossover points for internal consistency (Fig. 1). The Yellow Sea region provides an excellent test area for determining the accuracy of altimetric tidal information in coastal areas because of its semienclosed characteristics, shallow depths, and large tidal signals.

Sea surface height (SSH) measurements in coastal regimes such as those made by T/P and a corresponding database of in-water in situ measurements are required to better understand coastal dynamics. An important question concerns how accurately can T/P determine the main tidal constituents in coastal regimes. Better use of T/P as a scientific research tool can only be made after its measurements are assessed for accuracy against in situ measurements. This is an important step toward understanding the relation between the height measurements returned by the altimeter and the complex tides of the ocean and gaining confidence in their interpretation.

2. Background Return to TOC

As part of the T/P validation, extensive intercomparison studies, and orbit error assessments (Christensen et al. 1994 ; Tapley et al. 1994 ; Nerem et al. 1994) have been made. Comparisons between T/P altimetry and island tide gauge data have been made (Nerem and Koblinsky 1994 ; Mitchum 1994) and with inverted echo sounders equipped with pressure gauges (Teague et al. 1995). However, island tide gauges measurements can be adversely affected by the local environment, which includes topography, winds, and runoff. Circulation patterns around many islands are often very complex (Gordon and Hughes 1981 ; Pattiaratchi et al. 1987 ; Maul 1977), and shadowing of surface waves can significantly affect the surface patterns (Cram and Hanson 1974). Thus, using a tide gauge to calibrate an altimeter may not be straightforward, and the relation between open ocean SSH and tide gauge measurements may not be as strong as the relation between SSH and moored instruments (Roemmich 1990 ; Maul and Bushnell 1992). Comparisons of T/P ocean tide models to a network of 86 tide gauges made by Desai and Wahr (1995) revealed that the T/P ocean tide models have accuracies on the order of 2–3 cm. The T/P-derived global ocean tide models remove approximately 20 cm^2 more of the T/P-measured sea surface variance than the Cartwright and Ray (1991) tide model and show a 19 cm^2 and 15 cm^2 improvement over the Schwiderski (1980a ,b) and Cartwright and Ray (1991) tide models, respectively, when compared to tide gauge estimates of ocean tides. Accuracy assessments and intercomparisons of recent ocean tide models based on T/P altimetry were made by Andersen et al. (1995) and Shum et al. (1997) . Nearly all of these recent tide models provided improvements over the Cartwright and Ray (1990 , 1991) and Schwiderski (1980a ,b) models.

3. Measurements Return to TOC

TOPEX/Poseidon was launched 10 August 1992 as a joint effort by the U.S. National Aeronautics and Space Administration (NASA) and the French Space Agency, Centre National d'Etudes Spatiales (CNES), for studying global ocean circulation (Fu et al. 1994). The T/P data utilized in this study begin in late September 1992 and were obtained from the Geophysical Data Records (GDRs) processed at the Physical Oceanography Distributed Active Archive Center (PODAAC) at the Jet Propulsion Laboratory. TOPEX/Poseidon has a repeat period of 9.9156 days and an equatorial cross-track separation of 315 km. Data from T/P are corrected for the effects of wet troposphere from an onboard water vapor radiometer; dry troposphere, ionosphere from the dual-frequency altimeter, inverse barometer, and electromagnetic bias. The ionospheric correction is smoothed using a Gaussian filter with a rolloff of about 100-km along track. The height data are interpolated along track to a reference ground track produced at the Colorado Center for Astrodynamics Research, resulting in about 7-km spacing. Height observations from T/P are accurate to better than 3 cm rms (Fu et al. 1994). However, this accuracy is not generally achievable on the continental shelf with using only the Grenoble tide solution (LeProvost et al. 1994). A study by Jacobs et al. (1998) , also in the region, additionally removed empirically the eight principal tide constituents in order to improve the accuracy.

The tide gauge data from the eight coastal stations were obtained from the International Hydrographic Office database (IHO 1990). These stations were selected for their close proximity to T/P ground tracks. Distances from the tide gauges to the ground tracks range from 14 to 31 km. Much of these tide gauge data contain only the tidal coefficients for the M2, S2, O1, and K1 constituents. This study is limited to these four tidal constituents for consistency in combined analyses with the other measurements where more constituents could perhaps be determined. However, the four constituents account for about 80% of the tidal variability in this area, and thus provide a good estimation of the tidal heights.

The pressure gauges at moorings MA and MB (Fig. 1) are Sea-Bird Electronics Model 26 Seagauges. They are bottom-moored and have an accuracy of about 3 cm. The pressure measurements are referred to in units of meters since the pressure of 1 db corresponds approximately to the sea pressure exerted by a water column of 1 m. These moorings are within 3 km of T/P ground points and provide pressure measurements for July–October 1995.

4. Data comparisons Return to TOC

The T/P sea surface heights are compared with two moored pressure gauges (MA and MB) and eight coastal tide stations (S1–S8), and are intercompared at seven T/P crossover points (Fig. 1). Crossover points are at the intersections of ascending and descending ground tracks. For example, the crossover of T/P track T69 and T/P track T115 is indicated by an × near 35°N, 123°E in Fig. 1. The month of September (1995) is chosen due to the low to moderate winds during this period and the availability of the moored data. Tables 1–3 provide standard deviations (σ) of the pressure gauge tidal heights, tide station heights, and the T/P heights; correlations, standard deviation ratio (σ_1/σ_2), and tidal amplitude ratio (A_1/A_2) between various pairs of measurements; distance between measurements; number of valid T/P data points; and rms differences. Tidal amplitude is defined here as one-half of the maximum peak to trough distance. Subscripts 1 and 2 in the tables refer to the datasets identified in the table columns labeled data 1 and data 2. Pairs of datasets are selected from the tide station, T/P, and pressure gauge measurements.

Amplitudes and local phases for the individual constituents (M2, S2, K1, and O1) calculated from the tidal stations, pressure gauges, and T/P are given in Table 4. Local phases are sufficient for the internal comparisons in this paper. A more complete tidal analysis of the pressure gauge measurements is contained in Teague et al. (1998). A phase difference of 30° corresponds to a 1-h shift at the semidiurnal tidal frequency and a 2-h shift at the diurnal tidal frequency. The constituent M2 dominates the tidal height series except at the Bohai tide stations S4 and S7, and at the crossover of T69 and T39. Phase differences between comparisons are less than 1 h for the M2 constituent except for S7 at T69, located in the Bohai Sea. Similar phase differences are obtained for the S2 constituent, except for phase differences greater than 1 h for S4 at T39, also located in the Bohai Sea. The K1 amplitude is almost equal to the M2 amplitude at S4, and the K1 and O1 amplitudes are larger than the M2 amplitude at S7.

a. T/P tide estimates

Much work has been done to estimate tides from altimeter data for global deep water regimes (Egbert et al. 1994). Less work has been done on estimating tides locally in shallow water (Yanagi et al. 1996). In this paper, tides are determined via a harmonic analysis. To estimate tidal variability, a least squares fit is used to determine the eight principal tidal constituents (M2, S2, K1, O1, N2, P1, K2, and MU2) at each point along the ground track (Jacobs 1998). Only the first four tides are examined in this paper. In the Yellow and Bohai Seas, there are four ascending (T26, T39, T77, and T115) and three descending (T31, T69, and T107) T/P ground tracks. For this study, there are at most about 180 height estimates available at ground points for calculation of the tidal constituents. Generally, as the satellite approaches land, the last three to four height samples (about 7 km apart) contain fewer valid data measurements due to land effects. As the satellite flies from over land to over water, land effects are more severe, and the first five to six samples over water are degraded. TOPEX/Poseidon provides reasonable tide estimates for the Yellow Sea along the ground tracks, within about 20 km of land for ground tracks approaching land and within about 35 km for ground tracks coming off land. The number of valid measurements for each ground track as a function of latitude is shown in Fig. 2. An island, Haiyang Dao, not shown in Fig. 1, affects T77 near 39°N and an unknown obstacle affects T39 near 37.6°N, at a charted water depth of about 12 m. Varying low water conditions from land just northwest of the track may be causing data dropouts. The number of T/P data measurements used in the calculation of tides ranged from a low of 95 observations at tide station S2 to a high of 174 observations at moored pressure gauge MA.

b. T/P–Pressure gauge comparisons

Tidal heights from T/P and the moored pressure gauges for the month of September 1995 are presented in Fig. 3. There is good visual agreement between these measurements. Correlations are 0.99 and 0.98 and rms differences are 0.07 and 0.14 m for MA and MB with T/P, respectively. Good agreement in standard deviation of tidal heights between pressure gauge and T/P measurements is found at both mooring locations. Better agreement is found at the southernmost pressure gauge, MA, where the standard deviation ratio of MA/T26 is near unity (1.012). Standard deviations of heights at both moored pressure gauges are larger than those from T/P data. Amplitude ratios are near unity. Tidal amplitudes are slightly underestimated by T/P in comparisons with the pressure gauge measurements at the northern mooring, MB.

c. T/P–Tide station comparisons

Similar comparisons are made with T/P tidal heights and the coastal tide stations (Fig. 4). However, for these comparisons, the tide stations are not directly on the T/P ground tracks, lying off the ground tracks by 14–31 km. This causes some differences in amplitude and phase. In some cases, the closest T/P ground point (to S4 and to S7, both located in the Bohai Sea) does not contain sufficient valid data to calculate the tides. In general points with less than half the number of possible points were ill conditioned. The T/P ground points, which are farther away but contain enough valid data to calculate the tides, are used in these comparisons. Sufficient sampling is determined from an eigen-decomposition of the least squares matrix used in computing the tide coefficients and a comparison of the largest to smallest eigenvalues. If the ratio of the smallest to largest eigenvalues is too small, then the least squares problem is ill conditioned, and an accurate solution may not be obtained with the given sampling.

Both amplitude and phase at tide stations S1, S2, S5, S6, and S8 are in close agreement with T/P measurements. Amplitudes compare well but phases are off by several hours at tide station S3 (at T115). Amplitudes are underestimated by T/P at tide station S3 (at T107). Root-mean-square differences are large, 0.39 and 0.30 m, respectively. Since the distance from S3 to the T/P track is over 30 km for both cases, these kinds of discrepancies are not surprising for coastal regimes in which conditions can differ greatly over short distances. The nearby crossover comparison of T107 and T115 is very good with an rms difference of 0.06 m. High water amplitudes are overestimated by T/P (T69) at tide station S7 in the northern Bohai Sea. Agreement in amplitude and phase at tide station S4 in the southwestern Bohai Sea with T/P is poor. This comparison is suspect since T/P (T39) required 15 ground points to recover while coming off land, more than twice the usual number of 5 or 6 ground points. Standard deviation ratios range from 0.72 to 1.01, except for S3 at T107 where the ratio is 1.50 (Table 1). The T/P standard deviation of heights is generally greater than that from the tide stations. Amplitude ratios are less than unity for seven out of the nine comparisons as T/P estimated tidal amplitudes are greater than the tidal amplitudes calculated at the tide stations. TOPEX/Poseidon underestimates the tidal amplitude at just one case, S3 at T107. Shapes of the height time series are most different between pairs S4 at T39 and S7 at T69, and correlations are corresponding lower (0.85 and 0.92) than all other comparisons.

d. T/P crossover comparisons

Comparisons at the crossover points enhance the credibility of the T/P data. Intercomparisons of T/P at crossover points are favorable for both amplitude and phase except for the comparison of T69 at T39 in the Bohai Sea (

Fig. 5). Standard deviation and amplitude ratios are furthest from unity here, 0.902 and 0.903, respectively. At the other six crossover points, standard deviation ratios, amplitude ratios, and correlations are near unity (Table 3). Best agreement among all of the comparisons is found in the middle of the Yellow Sea at the crossover of T69 and T115 where the correlation is 1.0 and the rms difference is 0.04 m.

5. Discussion Return to TOC

Good approximations of the total tide height in the Yellow Sea are formed from the four main tidal constituents The predicted tide, T_p, is formed by combining these constituents. In order to estimate the contributions of the tides to the total variability, tidal residuals and normalized residuals are calculated. Residual tide rms σ_r, is given by

$$\sigma_r = \left[\frac{1}{T}\int_0^T (P_{\mathrm{pg}}(t) - T_p(t))^2\, dt\right]^{1/2}, \qquad (1)$$

for a time series of length T, where P_{pg} is the pressure gauge measurement. The normalized residual, σ_n, is defined as σ_r/σ_p, where σ_p is the standard deviation of the pressure measurements. The tidal residual is 14 cm for both MA and MB. Normalized residual is 0.25 for MA and 0.20 for MB. The normalized residuals reflect tidal contribution to the overall rms variability of about 75% and 80%, respectively.

TOPEX/Poseidon provides reasonable tide estimates for the Yellow Sea along the ground tracks. Comparisons are best between T/P and the pressure gauge measurements that are coincident with the ground track. Differences are larger in tide station comparisons with T/P, but all of the tide station measurements lay off the ground track. Cotidal charts generated from tide models indicate that the Bohai Sea and the western coast of Korea are regions of high tidal variability (Blain 1997). Tidal amplitudes and phases can change dramatically over short distances and can easily account for the larger differences in tide-station comparisons with T/P. Numerous tide measurement locations are required to understand these regions. The seven T/P ground tracks in the Yellow and Bohai Seas provide excellent coverage along track but limited coverage across track. Finer cross-track coverage is available from the *ERS-1* satellite whose ground tracks repeat only every 35 days, but the sun-synchronous orbit characteristic aliases most of the principal diurnal and semidiurnal tides to the annual and mean frequencies along repeat ground tracks. The 6-yr time series now available from T/P can be used to resolve the main tidal constituents.

Tide estimates from T/P are not as good in parts of the Bohai Sea as in the Yellow Sea. Reasons for the larger discrepancies in the Bohai Sea include nonlinear tide effects in this shallow sea, river effects, and decrease in dominance of the M2 and S2 tides. The Yellow River (Huang He) empties into the southwestern Bohai Sea near tide station S4 and is second in outflow to the Yangtze River (Changjiang River) in the Yellow and Bohai Seas. A large amount of silt is carried by the Yellow River. More T/P data dropouts are speculated to result from the surfacing of shallow water mud flats during low tide conditions. There is about a 12% decrease in the number of valid data points along T/P track T69 in the Bohai Sea. A similar number of valid data points are found along track T39 located entirely in the Bohai Sea.

In comparing the T/P height time series with the the tidal station and moored pressure gauge time series, standard deviations are computed and compared in addition to computing the rms of the difference between the two time series. Differencing of two time series of heights, which have similar amplitudes but small differences in phase, can lead to apparently large differences in amplitudes and is misleading. Thus overall statistics of each time series such as standard deviation and amplitude are included in this analysis.

6. Conclusions Return to TOC

Satellite altimetry can provide accurate along-track tidal estimates for the main tidal constituents in shallow coastal seas. Five years of T/P data provide good estimates in the Yellow and Bohai Seas of the M2, S2, K1, and O1 constituents. Here, higher accuracy is found in the Yellow Sea than in the Bohai Sea. The M2 and S2 tidal constituents in the Bohai Sea are less dominant than in the Yellow Sea, which suggests that more than the four tidal constituents analyzed here are required to provide good tide estimates in the Bohai Sea. Accurate tide estimates can be made to within about 20 km of the coast for T/P passes from over water to over land and to about 35 km of the coast for T/P passes from over land to over water.

Comparisons with in situ measurements are important in order to verify the accuracy of T/P data to measure tidal components in specific regions. Best tide estimates from T/P are made for ground points where data dropouts are few. Internal consistency in height determinations for the main tidal components at satellite crossover points suggest areas where accurate tide estimates are possible from altimetry. Comparisons of T/P tide estimates by various techniques are important to measure the accuracy of T/P data for determining tidal components.

Acknowledgments. This work was supported by the Office of Naval Research as part of the Basic Research Project "Yellow and East China Seas Experiment" under Program Element 601153N.

REFERENCES Return to TOC

Andersen, O. B., P. L. Woodworth, and R. A. Flather, 1995: Intercomparison of recent ocean tide models. *J. Geophys. Res.,* **100,** 25 261–25 282.

Blain, C. A., 1996: The role of assimilation station location in predicting the M2 and K1 tides in the Yellow Sea. Preprints, *Conf. on Coastal Oceanic and Atmospheric Prediction,* Atlanta, GA, Amer. Meteor. Soc., 60–67.

——, 1997: Development of a data sampling strategy for semienclosed seas using a shallow-water model. *J. Atmos. Oceanic Technol.,* **14,** 1157–1173.

Cartwright, D. E., and R. D. Ray, 1990: Oceanic tides from Geosat altimetry. *J. Geophys. Res.,* **95,** 3069–3090.

——, and ——, 1991: Energetics of global ocean tides from Geosat altimetry. *J. Geophys. Res.,* **96,** 16 897–16 912.

——, and ——, 1994: On the radiational anomaly in the global tide with reference to satellite altimetry. *Oceanol. Acta,* **17** (5), 453–459.

Choi, B. H., 1988: A fine grid two-dimensional M2 tidal model of the East China Sea. *J. Korean Assoc. Hydrol. Sci.,* **21** (2), 183–192.

Christensen, E. J., and Coauthors, 1994: Calibration of TOPEX/Poseidon at Platform Harvest. *J. Geophys. Res.,* **99,** 24 465–24 485.

Cram, R., and K. Hanson, 1974: The detection by ERTS-1 of wind-induced ocean surface features in the lee of the Antilles Islands. *J. Phys. Oceanogr.,* **4,** 594–600.

Desai, S. D., and J. M. Wahr, 1995: Empirical ocean tide models estimated from TOPEX/POSEIDON altimetry. *J. Geophys. Res.,* **100,** 25 205–25 228.

Egbert, G. D., A. F. Bennett, and M. G. G. Foreman, 1994: TOPEX/Poseidon tides estimated using a global inverse model. *J. Geophys. Res.,* **99,** 24 821–24 852.

Fu, L.-L., E. J. Christensen, C. A. Yamarone Jr., M. Lefebvre, Y. Menard, M. Dorrer, and P. Escudier, 1994: TOPEX/Poseidon mission overview. *J. Geophys. Res.,* **99,** 24 369–24 381.

Gordon, H. B., and R. L. Hughes, 1981: A study of rotating baroclinic nonlinear flow around an island, *J. Phys. Oceanogr.,* **11,** 1011–1014.

IHO, 1990: *Tidal Constituent Bank Station Catalogue.* International Hydrographic Bureau, 104 pp. [Available from the International Hydrographic Organization, Canadian Hydrographic Service, Ottawa, ON K1A 0E6, Canada.]

Jacobs, G. A., 1998: Sea surface height variations in the Yellow and East China Seas, Part 1. Linear response to local wind stress. *J. Geophys. Res.,* **103** (C9), 18 459–18 478.

——, R. H. Preller, S. K. Riedlinger, and W. J. Teague, 1998: Coastal wave generation in the Bohai Bay and propagation along the Chinese coast. *Geophys. Res. Lett.,* **25** (6), 777–780.

Kantha, L. H., C. Tierney, J. W. Lopez, S. D. Desai, M. E. Parke, and L. Drexler, 1995: Barotropic tides in the global oceans from a nonlinear tidal model assimilating altimetric tides 2. Altimetric and geophysical implications. *J. Geophys. Res.,* **100,** 25 309–25 317.

LeProvost, C. M., L. Genco, F. Lyard, P. Vincent, and P. Canceil, 1994: Spectroscopy of the world ocean tides from a finite element hydrodynamical model. *J. Geophys. Res.,* **99,** 24 777–24 798.

Maul, G. A., 1977: The annual cycle of the Gulf Loop Current. Part I: Observations during a one-year time series. *J. Mar. Res.,* **35** (1), 29–47.

——, and M. Bushnell, 1992: The relation between acoustic travel time and dynamic height anomaly off Abaco Island, Bahamas. Joint IAPSO-IOC Workshop on sea level measurements and quality control, Workshop Rep. 81. [Available from UNESCO, 7 place de Fontenoy, 75352 Paris 07 SP, France.]

Mitchum, G., 1994: Comparison of TOPEX sea surface heights and tide gauge sea levels. *J. Geophys. Res.,* **99,** 24 541–24 553.

Nerem, R. S., and C. J. Koblinsky, 1994: Monitoring of global sea-level variations using TOPEX/Poseidon altimeter data. *TOPEX/Poseidon Research News,* Vol. 2, 5–9. [Available from Jet Propulsion Laboratory, Pasadena, CA 91109.]

——, E. J. Schrama, C. J. Koblinsky, and B. Beckley, 1994: A preliminary evaluation of ocean topography from the TOPEX/Poseidon mission. *J. Geophys. Res.,* **99,** 24 565–24 583.

Nishida, H., 1980: Improved tidal charts for the western part of the north Pacific Ocean. *Rep. Hydrogr. Res.,* **15,** 55–70.

Ogura, S., 1933: The tides in the seas adjacent to Japan. *Bull. Hydrogr. Dept.*, **7,** 1–189.

Pattiaratchi, C., A. James, and M. Collins, 1987: Island wakes and headland eddies: A comparison between remotely sensed data and laboratory experiments. *J. Geophys. Res.,* **92,** 783–794.

Roemmich, D., 1990: Sea level and the thermal variability of the ocean. *Sea Level Change,* National Research Council, Eds., National Academy Press, 208–217.

Schlax, M. G., and D. B. Chelton, 1994: Aliased tidal errors in TOPEX/Poseidon sea-surface height data. *J. Geophys. Res.,* **99,** 24 761–24 775.

Schwiderski, E. W., 1980a: Ocean tides, Part I: Global ocean tide equations. *Mar. Geod.,* **3,** 161–217.

——, 1980b: Ocean tides, Part II: A hydrodynamical interpolation model. *Mar. Geod.,* **3,** 219–255.

Shum, C. K., and Coauthors, 1997: Accuracy assessment of recent ocean tide models. *J. Geophys. Res.,* **102,** 25 173–25 194.

Tapley, B. D., and Coauthors, 1994: Precision orbit determination for TOPEX/Poseidon. *J. Geophys. Res.,* **99,** 24 383–24 404.

Teague, W. J., Z. R. Hallock, G. A. Jacobs, and J. L. Mitchell, 1995:Kuroshio Sea surface height fluctuations observed simultaneously with inverted echo sounders and TOPEX/Poseidon. *J. Geophys. Res.,* **100,** 24 987–24 994.

——, H. T. Perkins, Z. R. Hallock, and G. A. Jacobs, 1998: Current and tide observations in the Southern Yellow Sea. *J. Geophys. Res.,* **103,** 27 783–27 793.

Yanagi, T., A. Morimoto, and K. Ichikawa, 1996: Co-tidal and co-range charts for the East China Sea and Yellow Sea derived from satellite altimetry data. Oceanographic study in the East China Sea and the Yellow Sea by the MASFLEX project. Ehime University Dept. of Civil and Ocean Engineering Report, 181 pp. [Available from Dept. of Civil and Ocean Engineering, Ehime University, Matsuyama 790-8577, Japan.]

Figures Return to TOC

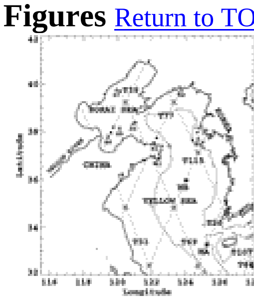

Click on thumbnail for full-sized image.

Fig. 1. Location of pressure gauge moorings (MA and MB; squares), tide stations (S1–S8; triangles), T/P ground tracks (T77 for example; dotted lines), T/P comparison points (large dots), and T/P crossover points (×'s). Depth contours for 50 and 100 m are shown.

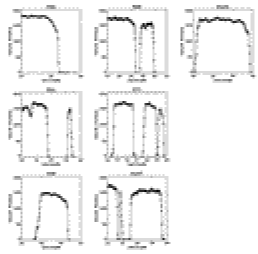

Click on thumbnail for full-sized image.

Fig. 2. Number of valid data points along ascending ground tracks 26, 39, 77, and 115, and descending ground tracks 31, 69, and 107, as a function of latitude.

Click on thumbnail for full-sized image.

Fig. 3. Comparison of pressure gauge time series (thick lines) with T/P (thin lines). Note that the lines nearly overlay.

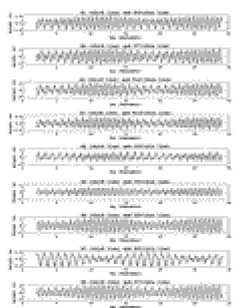

Click on thumbnail for full-sized image.

Fig. 4. Comparison of tide station time series (thick lines) with T/P (thin lines).

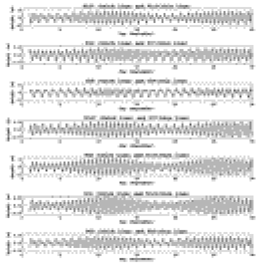

Click on thumbnail for full-sized image.

Fig. 5. Comparison of T/P time series at crossover points.

Corresponding author address: Mr. William J. Teague, Meso- and Finescale Ocean Physics Section, Department of the Navy, Naval Research Laboratory, Stennis Space Center, MS 39529-5004.
E-mail: teague@nrlssc.navy.mil
* NRL SSC Contribution Number JA7332-99-0001.

Tables Return to TOC

Table 1. Tide stations and T/P.

Data 1	Data 2	Correlation	σ_1 (m)	σ_2 (m)	σ_1/σ_2	A_1/A_2	Dist (k
S1	T69	0.97	0.664	0.761	0.872	0.854	30
S2	T77	0.96	0.473	0.501	0.946	0.972	27
S3	T107	0.99	0.855	0.572	1.495	1.472	30
S3	T115	0.93	0.855	1.032	0.829	0.836	31
S4	T39	0.85	0.242	0.334	0.724	0.675	23
S5	T39	0.94	0.283	0.279	1.014	0.955	31
S6	T69	0.98	0.448	0.520	0.862	0.849	14
S7	T69	0.92	0.211	0.239	0.882	0.841	19
S8	T77	1.00	1.429	1.420	1.007	1.022	22

Table 2. Moored pressure guages and T/P.

Data 1	Data 2	Correlation	σ_1 (m)	σ_2 (m)	σ_1/σ_2	A_1/A_2	Dist (k
MA	T26	0.99	0.548	0.541	1.012	0.999	2
MB	T115	0.98	0.741	0.691	1.072	1.059	2

Table 3. T/P at crossover points.

Data 1	Data 2	Correlation	σ_1 (m)	σ_2 (m)	σ_1/σ_2	A_1/A_2	T/P c
T107	T115	1.00	0.793	0.838	0.946	0.934	1
T31	T77	0.99	0.621	0.645	0.963	0.981	16
T69	T39	0.95	0.270	0.299	0.902	0.903	1
T107	T77	1.00	1.169	1.171	0.998	1.027	1
T69	T115	1.00	0.492	0.484	1.017	1.031	17
T31	T115	1.00	1.260	1.181	1.067	1.077	1
T69	T26	1.00	0.565	0.562	1.007	1.026	17

Table 4. Tidal amplitudes (m) and phases (°).

		M2:DATA1	M2:DATA2	S2:DATA1	S2:DATA2
Data 1	Data 2	Amp/Phase	Amp/Phase	Amp/Phase	Amp/Phase
MA	T26	0.68/−104.0	0.69/−108.0	0.29/2.0	0.25/−10.0
MB	T115	0.95/155.0	0.89/146.0	0.38/−124.0	0.32/−136.0
S1	T69	0.88/141.0	0.99/133.0	0.15/−149.0	0.32/−137.0
S3	T115	1.08/58.0	1.31/81.0	0.37/137.0	0.48/158.0
S6	T69	0.61/−99.0	0.69/−90.0	0.17/−35.0	0.23/−20.0
S2	T77	0.60/−103.0	0.66/−88.0	0.18/−28.0	0.16/−18.0
S4	T39	0.22/−99.0	0.39/−124.0	0.07/−32.0	0.17/−82.0
S7	T69	0.11/−127.0	0.05/162.0	0.03/−60.0	0.07/−37.0
S3	T107	1.08/58.0	0.70/64.0	0.37/137.0	0.28/143.0
S5	T39	0.38/−109.0	0.34/−124.0	0.11/−42.0	0.16/−61.0
S8	T77	1.90/−45.0	1.87/−43.0	0.55/30.0	0.61/32.0
T107	T115	1.02/101.0	1.06/100.0	0.38/−179.0	0.40/178.0
T31	T77	0.82/17.0	0.85/19.0	0.18/94.0	0.16/109.0
T69	T39	0.23/−145.0	0.32/−148.0	0.12/−59.0	0.13/−66.0
T107	T77	1.53/−46.0	1.55/−45.0	0.50/30.0	0.46/29.0
T69	T115	0.64/178.0	0.64/180.0	0.25/−90.0	0.21/−95.0
T31	T115	1.63/−142.0	1.55/−139.0	0.69/−53.0	0.60/−52.0
T69	T26	0.70/−89.0	0.71/−88.0	0.32/8.0	0.31/8.0